Fluid Pinch-Off Dynamics at Nanometer Length Scales

J. C. Burton, J. E. Rutledge, and P. Taborek

Department of Physics and Astronomy, University of California, Irvine, California 92697, USA

The breakup of a drop of inviscid fluid into two smaller drops is determined by a competition between surface and inertial forces. This process forms a thin filament of fluid with a connecting neck that shrinks to zero diameter at a finite time singularity. We present measurements of the electrical resistance of a liquid bridge of mercury as it undergoes pinch off. The electrical measurements allow us to probe the region of the singularity down to nanosecond times and nanometer lengths. Near pinch off, the resistance of the liquid bridge diverges as $t^{-2/3}$, as expected for inviscid flow.

PACS numbers: 47.55.Dz, 47.20.Dr

Capillary pinch off in fluids has been of recent interest because of its technological importance and because it is a simple example of a system that displays a spontaneous finite time singularity [1–5]. When gravitational forces are negligible, a fluid droplet in static equilibrium forms either a sphere or a spherical cap if it is attached to a surface. For a sufficiently strong perturbation of the droplet shape, two separate droplets with spherical surfaces form. The dynamical process by which the fluid changes its topology and transforms into two distinct pieces typically involves the formation of a long slender filament of fluid that connects the two nascent droplets. Surface tension drives flows that shrink the diameter of the filament in a nonuniform way and eventually lead to pinch off in a neck region. The dynamics of this process is governed by the nonlinear Navier-Stokes equations. Near the singularity in the neck region, the solutions have a relatively simple self-similar form that can be characterized by power laws. There are two types of generic behavior distinguished by the value of the dimensionless ratio $Oh = \eta/\sqrt{\rho d \sigma}$, where σ is the surface tension, ρ is the density, η is the viscosity, and d is the neck diameter. For $Oh > 1$, inertia is negligible, and the flow results from a balance between surface tension and viscous forces, which leads to an asymptotic linear relationship between d and τ, the time remaining until pinch off:

$$d \propto \frac{\sigma \tau}{\eta}. \tag{1}$$

This is known as the viscous thread regime and has been studied by numerous authors [4,6–11]. For $Oh < 1$, the effects of viscosity are negligible, and the flow is a balance between surface tension and inertia. For this case of inviscid potential flow, dimensional analysis yields a different relationship between τ and d:

$$d \propto \left(\frac{\sigma \tau^2}{\rho}\right)^{1/3}. \tag{2}$$

The characteristic neck size d is a function of τ, with $d \to 0$ as $\tau \to 0$, so Oh can span a wide range of values during a pinch-off flow. This analysis suggests that even if

Oh is initially small, as $d \to 0$ there will be a transition to a viscously dominated regime near $\tau = 0$. This transition has been observed using viscous mixtures, but for simple fluids such as helium [12], water [1], or mercury, the crossover to viscous behavior is not expected to occur until d reaches molecular dimensions where the validity of the continuous fluid description breaks down. In particular, pinch off in mercury droplets should be described by the potential flow equations analyzed in [13,14] and are expected to obey the scaling law of Eq. (2), even for neck dimensions d of molecular size.

Pinch off in the potential flow regime has typically been studied using strobe photography and high-speed video [1,4,5,12,15,16]. The spatial resolution of these imaging techniques is limited by the conventional constraints of optical instrumentation, but, even more importantly, both experiment [1] and computer simulation [13] show that the profile of an inviscid pinch is reentrant, and resembles the region near the stem of an apple, as shown in Fig. 1. This means that the singularity in the
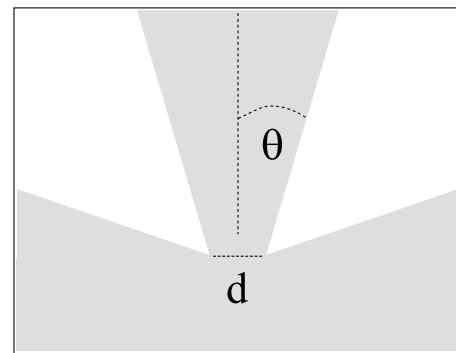

FIG. 1. A schematic diagram showing a cross section of the neck region close to pinch off for an inviscid fluid. The liquid filament attaches to the lower droplet at a point below the horizon formed by the droplet, and is not visible using standard projection imaging techniques. The electrical resistance of the filament is determined by the minimum neck diameter d and the cone angle θ. Although θ is not directly measured in our experiment, both theory and observation indicate that $\theta \sim 18°$, as described in the text.

neck occurs below the horizon formed by the reentrant part of the drop, and is inaccessible to conventional imaging techniques. For this reason, previous optical measurements of inviscid pinch off have been limited to the range $d > 50$ μm [1]. We have developed a technique that avoids the problem of the reentrant profile by monitoring the electrical resistance of a conducting fluid (Hg) during pinch off. This experimental method extends the spatial range of observation of potential flow pinch off by more than 3 orders of magnitude over previous optical measurements.

The connection between the measured electrical resistance and the geometry of the fluid filament relies on the observation that, near the singular region, the fluid filament has a conical shape as illustrated in Fig. 1. This type of conical cross section has been observed in experiment and computer simulations [13], and can also be seen in the photograph of Fig. 2. The effective electrical resistance R of a structure like that in Fig. 1 is well known [17] to be inversely proportional to the diameter of the narrowest constriction d. In the limit of small d, the resistance is independent of length and is given by

$$R = \frac{2\rho_r \cot(\theta)}{\pi d}, \qquad (3)$$

where ρ_r is the resistivity of the material and θ is the cone angle. In the analysis of our data, we also assume that d varies with time but θ does not; i.e., the cone has an invariant self-similar shape. This implies that the divergent behavior of R is determined by the singular behavior of the minimum neck diameter d, and θ affects only the amplitude of the singularity. Although there is no direct experimental verification of this assumption, numerical calculations for inviscid fluids [1,13] show that the shape of the pinch region near the singularity is independent of the initial flow conditions and approaches a conical shape with a universal value of $\theta \sim 18°$ as the neck diameter shrinks to zero.

Our experiments were conducted with liquid mercury at room temperature with pinch off occurring in air. Mercury was chosen due to its high electrical conductivity ($\rho_r = 96 \times 10^{-8}$ Ω m) and high available purity [18]. Other important physical properties are $\eta = 1.526$ cP, $\rho = 13.59$ g/cm^3, and $\sigma = 485.5$ dyn/cm at room temperature [18]. In order to maintain electrical contact at both ends of the liquid filament, we used a liquid bridge geometry [14,19]. This consisted of two 0.25 in. diameter copper rods with amalgamated end faces so that mercury would wet the flat surfaces (but not the curved surfaces) of the rods. The copper rods were mounted vertically with a small gap between the end faces. For small separations between the ends, a stable hour glass shaped bridge of mercury can be formed by capillary action. When the separation between the ends of the rods is increased, the bridge becomes unstable under the influence of surface

tension and forms a filament (Fig. 2), which eventually undergoes pinch off and breaks; the final state is two approximately hemispherical droplets, with one on each end face. In the absence of gravity, the pinch-off process maintains the symmetry of the initial hour glass, and there are two separate but simultaneous pinch regions, with one near each hemisphere. The gravitational capillary length $\sqrt{2\sigma/\rho g}$ is approximately 0.4 cm in mercury at room temperature, so gravity is negligible for flows on shorter length scales and is certainly unimportant near the singularity. Gravity does play a role, however, in the initial stages of this experiment by breaking the hour glass symmetry: this causes the fluid filament to pinch off at the lower hemisphere before it pinches near the upper hemisphere, as can be seen in the photograph in Fig. 2. Thus, the singularity in the electrical resistance of the mercury is determined by the hydrodynamics near the lower hemisphere alone.

The electrical resistance of the mercury was measured using a voltage biased voltage divider made up of the mercury filament and the 50 Ω input to an oscilloscope, as shown in Fig. 3. Since information about the behavior of the fluid at small length scales occurs at short times and high frequencies, considerable care was taken to simplify the high frequency response of our measuring circuit. In particular, input cables that represent a parasitic inductance and capacitance, were essentially eliminated by building the mercury drop electrodes into
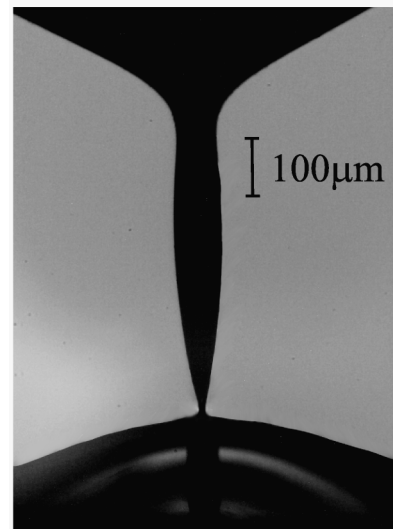

FIG. 2. High-speed photograph of a liquid mercury bridge, illuminated from behind, approximately 5 μs before pinch off. The upper and lower droplets of fluid are attached to the end of copper rods (not visible in the picture). Note that the thin filament which forms between the two bodies of fluid is slightly asymmetric and is narrower in the region near the bottom drop than near the upper drop. The reentrant shape shown in Fig. 1 occurs on very short length and time scales and cannot be seen in this type of image.
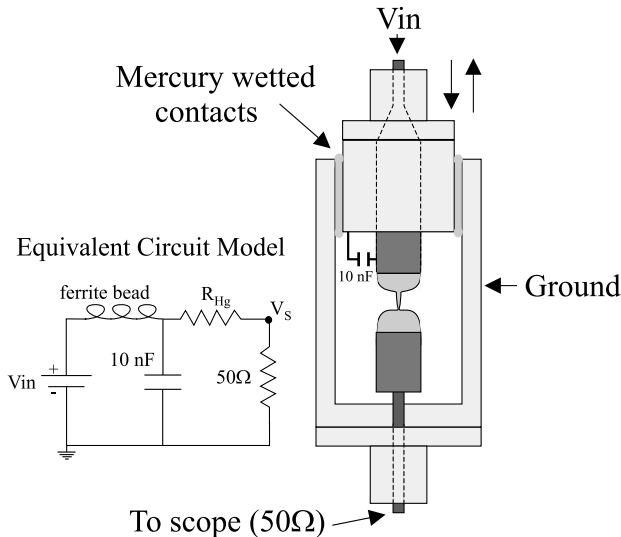
FIG. 3. Schematic cross section of the experimental apparatus. The copper rods that contact the mercury are surrounded by and electrically isolated from a copper coaxial ground. The upper copper electrode can slide in the vertical direction. Contact to ground during sliding is maintained by the mercury wetted contacts shown in the figure. The equivalent circuit on the left shows the resistance of the mercury filament R_{Hg} and the voltage detected by the oscilloscope V_s. V_{in} is provided by a power supply and has a nominal value of 1 V. The 50 Ω resistor is the input impedance of the scope.

a BNC connector that was connected directly into the input of the scope, so that the effective cable length was less than 2 cm. The bottom electrode was fixed, but the gap could be adjusted by moving the upper electrode in a coaxial fitting with mercury wetted contacts. The power supply that established the voltage bias V_{in} was decoupled from radio frequencies by placing a high inductance ferrite bead at the positive terminal of the power supply, and a large (≈ 10 nF) capacitor as close as possible to the upper body of mercury. The purpose of these additions to the circuit were to keep V_{in} constant independent of the value R_{Hg}. This was verified by a direct measurement of V_{in}, which was found to vary by less than 1% throughout the pinch-off process. The apparatus was connected directly to the input of a Tektronix TDS5000 oscilloscope with 5×10^9 samples/s and a 1 GHz bandwidth. The high frequency response of the circuit was checked by separating the rods so that the circuit was open, and then bringing the electrodes together to close the circuit. This procedure does not involve a fluid filament and is very fast. The observed response was a step function with a rise time of approximately 1 ns.

The pinch-off experiments were conducted by reversing this process, i.e., by starting from the closed circuit formed by the mercury bridge and retracting the upper electrode until the circuit was open. As the resistance of the mercury filament diverges, the voltage at the scope

input falls to zero, which provides the trigger for the event. A sample trace from the oscilloscope is shown in Fig. 4. Useful data could be obtained for a range of τ (the time before the break) of about 1 μs; for longer times the resistance of the filament was too small to distinguish from zero. Data such as that in Fig. 4 were independent of the speed of retraction of the upper electrode and were reproducible to within the width of the curve. The only exception to this occurred when the mercury was exposed to the air for more than a day and became contaminated with oxide. To avoid these problems, the experiments were conducted with 99.9999% pure electronic grade mercury freshly extracted from the interior of bulk fluid using a syringe.

The resistance of the fluid filament was obtained from the scope voltage using the circuit model shown in Fig. 3, with $R_{Hg} = 50(\frac{V_{in}}{V_s} - 1)$. The resistance measurements for all times before the trigger were fit using a power-law model with $R_{Hg} = A(t_{break} - t)^b$, where optimal values of the amplitude A, the exponent b, and the exact time of the singularity t_{break} were chosen using a χ^2 minimization procedure. The resistance data can be related to the minimum neck diameter d using Eq. (3), assuming that $\theta = 18°$ and that the resistivity has its bulk value. Figure 5 shows a log-log plot of d as a function of τ together with the best fit line, showing over three decades of power-law behavior. The best fit for the exponent that governs the time dependence of d is 0.661 ± 0.008, where the uncertainty represents the 95% confidence interval; this is consistent with the value predicted by the inviscid potential flow model $d \propto \tau^{2/3}$. The highest resistance that could be resolved in the measurements was about 340 Ω, which corresponds to a neck diameter of 2.7 nm. In contrast, the geometry captured in conventional optical images such as Fig. 2 corresponds to resistances of a fraction of an ohm, and diameters that are more than an
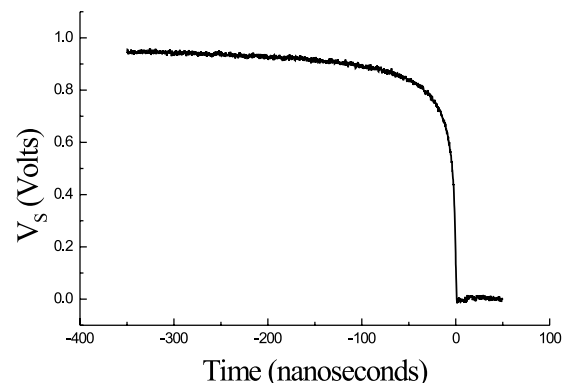

FIG. 4. Sample trace of the voltage V_s across the scope as a function of time during the last 0.5 μs before pinch off. The feature near $t = 0$ corresponds to the actual break point where the resistance goes to infinity and the voltage drops to zero; this was used to trigger the scope.
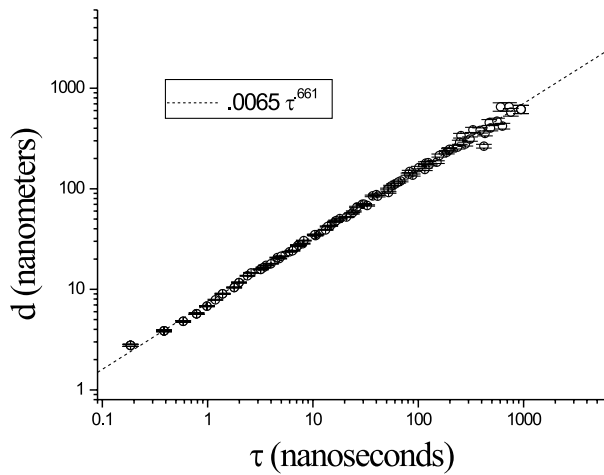
FIG. 5. Neck diameter d vs the time remaining until pinch off τ, showing a power law dependence over a wide range. The error bars represent the standard deviation of the shot-to-shot repeatability of the measurements. The dotted line and the inset show a least squares best fit.

order of magnitude larger than the largest ones appearing in Fig. 5.

In summary, we have developed a new experimental technique for studying pinch off in conducting fluids. This method overcomes the limitations of optical imaging and allows us to monitor the time dependence of the geometry of fluid filaments in the micrometer to nanometer range. This complements the millimeter to 10 μm range accessible with optics. We have verified that the power laws deduced on the basis of inviscid hydrodynamics continue to be obeyed down to pinch diameters of less than 5 nm. This analysis relies on the assumption of self-similarity of the geometrical shape of the singular region. The accuracy of power laws we observe over nearly four decades is strong experimental support for this assumption. Possible effects due to viscosity or nonconventional conduction mechanisms apparently are not important in this range.

[1] A. U. Chen, P. K. Notz, and O. A. Basaran, Phys. Rev. Lett. **88**, 174501 (2002).
[2] D. Leppinen and J. R. Lister, Phys. Fluids **15**, 568 (2003).
[3] A. Rothert, R. Richter, and I. Rehberg, New J. Phys. **5**, 59.1 (2003).
[4] I. Cohen and S. R. Nagel, Phys. Fluids **13**, 3533 (2001).
[5] A. Rothert, R. Richter, and I. Rehberg, Phys. Rev. Lett. **87**, 084501 (2001).
[6] M. P. Brenner, J. R. Lister, and H. A. Stone, Phys. Fluids **8**, 2827 (1993).
[7] D. T. Papageorgiou, Phys. Fluids **7**, 1529 (1995).
[8] J. Eggers, Phys. Fluids **7**, 941 (1995).
[9] W. W. Zhang and J. R. Lister, Phys. Rev. Lett. **83**, 1151 (1999).
[10] Y. Amarouchene, D. Bonn, J. Meunier, and H. Kellay, Phys. Rev. Lett. **86**, 3558 (2001).
[11] P. Doshi, I. Cohen, W. W. Zhang, M. Siegel, P. Howell, O. Barasan, and S. R. Nagel, Science **302**, 1185 (2003).
[12] J. C. Burton, P. Taborek, and J. E. Rutledge, J. Low Temp. Phys. **134**, 237 (2004).
[13] R. F. Day, E. J. Hinch, and J. R. Lister, Phys. Rev. Lett. **80**, 704 (1998).
[14] Y. J. Chen and P. H. Steen, J. Fluid Mech. **341**, 245 (1997).
[15] I. Cohen, M. P. Brenner, J. Eggers, and S. R. Nagel, Phys. Rev. Lett. **83**, 1147 (1999).
[16] X. D. Shi, M. P. Brenner, and S. R. Nagel, Science **265**, 219 (1994).
[17] J. D. Romano and R. H. Price, Am. J. Phys. **64**, 1150 (1995).
[18] *CRC Handbook of Chemistry and Physics*, edited by D. R. Lide (CRC Press, Boca Raton, FL, 2004), 84th ed.
[19] X. Zhang, R. S. Padgett, and O. A. Basaran, J. Fluid Mech. **329**, 207 (1996).